Biochimica et Biophysica Acta, 987 (1989) 8–14
Elsevier

BBAMEM 74548

Estimation of Na^+ dwell time in the gramicidin A channel. Na^+ ions as blockers of H^+ currents

Stefan H. Heinemann [1,2] and Frederick J. Sigworth [2]

[1] *Max-Planck-Institut für biophysikalische Chemie, Abteilung Membranbiophysik, Göttingen (F.R.G.) and* [2] *Department of Cellular and Molecular Physiology, Yale University School of Medicine, New Haven, CT (U.S.A.)*

(Received 6 July 1989)

Key words: Gramicidin A; Open channel noise; Channel block; Sodium ion transport; Proton transport

The permeation of Na^+ through gramicidin A channels shows a simple saturation with increasing Na^+ concentration that can be described by two different models. The first model assumes that one Na^+ binds to the channel with high affinity ($\approx 30\ M^{-1}$) and that conduction occurs by a 'knock-on' mechanism requiring double occupancy of the channel; the other model assumes that Na^+ binding is of low affinity ($< 1\ M^{-1}$), and that double occupancy of the channel is rare. NMR measurements have shown tight Na^+ binding, favoring the first model, but measurements of flux ratios and water transport support the second model. We present here a relatively model-independent measurement of the dwell time of Na^+ inside the channel, in which we characterize the fluctuations in H^+ current through the channel induced by 'block' from the more slowly permeating Na^+ ions. The mean Na^+ dwell time inside the channel is estimated to be ≈ 10 ns at a membrane potential of 200 mV. This result is inconsistent with tight Na^+ binding, thus favoring the second model.

Introduction

The permeation of monovalent cations through the gramicidin A channel appears to involve the binding of ions to sites near the end of the channel and their translocation across a central barrier (see, for example, Refs. 1 and 2). The details of permeation by Na^+ have been in some dispute. The concentration dependence of Na^+ conductance shows a simple saturation which, surprisingly, can be described equally well by two very different sets of rate constants. In one case, a relatively high affinity of Na^+ for the channel ($\approx 30\ M^{-1}$) would cause the channel to conduct predominantly by a 'knock-on' process involving double occupancy; saturation would occur when two ions are bound in the channel. In the other case, low affinity of Na^+ for the channel would cause it to act as a classical 'one ion' channel, with saturation corresponding to the occupation of one of the binding sites. Supported by ^{23}Na nuclear magnetic resonance (NMR) experiments, Urry et al. [3,4] proposed a tight binding of the first sodium ion of 30–100 M^{-1}; experiments with gramicidin analogues having a reduced number of amino acids also indicated that the gramicidin A channel becomes doubly occupied by sodium ions [5]. Finkelstein and Andersen [1], however, concluded from analysis of the concentration dependence of conductance, current-voltage relationships, and flux ratios that the first Na^+ binds very loosely ($\ll 1\ M^{-1}$) and that double occupancy does not occur.

The set of rate constants as proposed by Finkelstein and Andersen [1] is now widely accepted, but it is of interest to attempt to distinguish between the 'tight binding' and 'weak binding' theories by measuring the dwell time of Na^+ in the channel. By analogy with the work of Lansman et al. [6] in calcium channels, in which blockages of Na^+ current by calcium ions was used to estimate the affinity of calcium for the channel, we wished to find experimental conditions under which the sodium ions could be considered as a blocking agent for a probe current. Hydrogen ions have a very high, essentially diffusion-limited, permeability in GA channels [7] and serve as an ideal probe current carrier since only low concentrations of H^+ are needed to produce substantial currents and the dwell time of H^+ in the channel is very short. Together, these properties allow specific ion–ion interactions to be neglected, and the dwell time of a sodium ion in the channel can be considered as a slow blocking event for the much faster proton transport process.

Correspondence: S.H. Heinemann, Max-Planck-Institut für biophysikalische Chemie, Abteilung Membranbiophysik, Am Faßberg, D-3400 Göttingen, F.R.G.

The blocked times we would expect to observe, even in the case of tight Na^+ binding, are well below 1 μs and therefore would not be directly resolvable as interruptions in the single-channel H^+ current. However, as we have shown in the case of nanosecond-duration blockage of the gramicidin A channel by formamide [8], analysis of changes in the mean current and the open-channel noise with blocker concentration allows an estimate of the blocked time. Our experimental results are in support of a weak binding of sodium ions inside the gramcidin A channel.

Experimental methods

Micro-bilayers from glycerol monooleate (GMO) (NuCheck Prep, Elysian, MN, U.S.A.) 40 mg/ml in squalene (Sigma, St.Louis, MO, U.S.A.) were formed on the tips of borosilicate pipettes (Kimax-51, Kimble Products, Vineland NJ, U.S.A.) as described by Sigworth et al. [9]. H^+ current measurements were performed in symmetrical solutions of 20 mM and 80 mM HCl (pH 2.2 and 1.7, respectively) and a specified concentration of NaCl at room temperature (21°C). Under the same experimental conditions Na^+ currents were recorded at neutral pH. Purified gramicidin A was kindly provided by Prof. D.W. Urry.

Membrane currents were measured with an EPC-7 patch-clamp amplifier (List Medical, Darmstadt, F.R.G.), digitized, and stored on video tape at 44.1 kHz sampling rate. For further processing, 180-s stretches of data were transferred digitally to a disk file in a PDP 11/73 computer (Digital Equipment Corp., Marlboro, MA, U.S.A.). The digital data processing including filtering, masking of brief channel closings, calculation of the power spectra, and corrections for the system response function and artifacts due to channel gating have been described earlier [8–10]. For each experiment determinations were made of the mean single-channel current, i, and the average spectral density, S, which was obtained by averaging the power spectrum between 1 and 10 kHz. In some cases a slight decay of the spectra with frequency was found. In order to estimate the asymptotic shot noise level the spectra showing such a decay were fitted by the sum of a constant and a small component proportional to $1/f$ in the rage between 0.1 and 20 kHz. Since the values of the constant component were repeatable, we used them as measures of the ion transport noise for further calculations.

Characterization of the ion transport

Frehland [11,12] has shown that, given a discrete kinetic scheme for the transport of ions through a channel, the single-channel current i and also the spectral density S of the current fluctuations can be calculated. Our numerical implementation of this theory and its application to channel-blocking events has been described [8]; we summarize here its application to the transport of H^+ in the presence of Na^+.

Model-independent description

We first consider a simplified approach to the calculation of the mean channel current and spectral density. The current through a gramicidin A channel carried by a single permeant ion species shows, within the frequency range accessible to our measurements, a constant spectral density similar in magnitude to that predicted for a simple shot process [13],

$$S_H = 2q\, i_H\, r_H \tag{1}$$

and

$$S_{Na} = 2q\, i_{Na} r_{Na} \tag{2}$$

where q is the elementary charge ($1.6 \cdot 10^{-19}$ C). The factors r_H and r_{Na} are equal to unity in the case of a unidirectional flux of independently-moving ions that encouter only one rate-limiting step in translocation across the membrane; we introduce these factors here to account phenomenologically for the concentration-dependent correlation among individual ion transport events [8,14].

We now introduce an interaction between Na^+ and H^+ currents, such that current carried by one ion species cannot flow while one of the other ion species is inside the channel. The mean current i is the sum of Na^+ current and the H^+ current

$$i = i_{Na} + i_H \tag{3}$$

The proton current is given by

$$i_H = \frac{i_H^0}{(1 + c_{Na}\lambda\tau)} \tag{4}$$

where i_H^0 is the current carried by protons in the absence of sodium ions, c_{Na} is the sodium concentration, λ is the entry rate of sodium ions, and τ is their mean dwell time in the channel.

The sodium current i_{Na}^0 in the absence of protons can be estimated from independent experiments at various Na^+ concentrations and at neutral pH. The H^+–Na^+ interactions, however, will result in a reduction of i_{Na}. Given the ratio ρ of the mobilities of Na^+ and H^+ inside the channel, one can approximate i_{Na} by

$$i_{Na} \approx \frac{i_{Na}^0}{\rho i_H + i_{Na}^0}. \tag{5}$$

As a first approximation ρ can be assumed to be close to 0.1 [7].

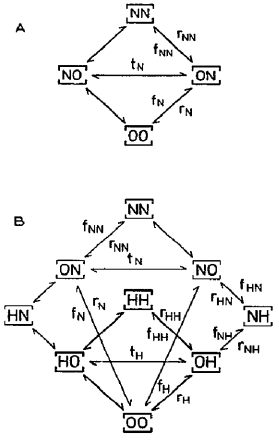

Fig. 1. Kinetic schemes for ion transport in the gramicidin A channel. (A) Four-state scheme for a channel with two binding sites. At low ion concentrations the transport of the ion (N) is represented by cyclic transitions in the lower half of the diagram, as the empty channel [00] binds an ion [N0] which is then translocated [0N] and dissociates. At high concentrations the transport consists of cyclic transitions in the upper half of the diagram. (B) Nine-state scheme for transport in the presence of both H^+ and Na^+. The four states for H^+-transport alone are drawn with heavy lines.

The spectral density of the current fluctuations with both H^+ and Na^+ present is approximated by [8]

$$S \approx S_{Na} + S_H + 4c_{Na}\lambda\tau^2 i_H^2 \qquad (6)$$

The last term accounts for the noise generated by the interruptions of proton flow by the presence of a sodium ion inside the channel. It should be pointed out that Eqns. 4 and 6 only hold if there are no specific interactions of protons with sodium ions, if the dwell time of Na^+ inside the channel is much larger than the dwell time of H^+ (i.e., $\rho \ll 1$), and if the total reduction of the proton current by sodium ions is small (i.e., λ, τ small). Provided that the sodium ions have a high affinity to the gramicidin A channel, i.e., τ is large, one would expect a reduction in mean current and an increase in spectral density as c_{Na} is increased.

TABLE I

Rate constants of a 2S3B model (Fig. 1A) for the proton transport through gramicidin A in s^{-1}

The rate constants are derived from experiments in GMO/squalene membranes (Fig. 3A,B).

Rate	Value
f_H/c	$2.2 \cdot 10^9$
r_H	$2.3 \cdot 10^7$
f_{HH}/c	$1.1 \cdot 10^9$
r_{HH}	$1.1 \cdot 10^{10}$
t_H	$2.0 \cdot 10^8$

Extended ion transport model

More straightforward, but also more involved, is the description of this discrete transport system by master equations and fluctuations about their solutions as introduced by Frehland [11,12]. For the application of this theory one must start with a specific kinetic model for the ion transport mechanism. We start with the 2-site, 3-barrier model (2S3B) of Finkelstein and Andersen ([1]; Fig. 1A) for proton conduction, and accomodate the flux of sodium by extending this model to nine states allowing sodium ions to compete with protons for the same binding sites (Fig. 1B). From an extensive number of experimental measurements of ion flow in solutions containing Na^+ and mixtures of H^+ and Na^+ one might be able to estimate all of the parameters in this scheme. We have not attempted to do this, but instead have used calculations based on sets of rate constants from the literature as a comparison of the predictions of this model (Table II).

Results

Na^+ transport: two models give identical predictions

Fig. 2A shows values of i obtained at 200 mV membrane potential as a function of Na^+ concentration; the data plotted as squares were taken from Neher et al. [15]. Superimposed are fitted curves calculated from the four-state model of Fig. 1A. For the solid curve the starting values of the fit were the 'weak binding' rate constants of Finkelstein and Andersen [1], while for the dotted curve the 'tight binding' values of Urry et al. [3,4] were used. The fitted values (listed in Table II) are very similar to the starting values, and fit the experimental points indistinguishable well even though two of the rate constants differ by two orders of magnitude between the two sets. The two sets of rate constants also predict essential identical current-voltage relations at 100 mM and 1 M Na^+ (Fig. 2E).

Fig. 2B compares the predicted concentration dependence of the spectral density with experimental data at Na^+ concentrations of 100 mM and 1 M. Again, the two sets of parameters yielded similar predictions, such that we would not be able to distinguish between the two models even if we could reliably measure the spectral density over a wide concentration range. For reference we include in Figs. 2C and 2D the concentration dependence of channel occupancy predicted from the two sets of rate constants. For weak Na^+ binding (Fig.

2C) curves for the probability of an empty channel and one ion bound are shown; saturation of the current occurs as the channel becomes singly occupied. In the case of tight Na^+ binding (Fig. 2D) it can be seen that the transition to double occupancy (shaded region) is responsible for the saturation of the current-concentration curve.

Characterization of proton transport

The two models for Na^+ transport make appreciably different predictions for i at very low Na^+ concentrations, but measurement of the single-channel current is difficult under such conditions. Instead we chose to measure the modulation of a H^+ current by low Na^+ concentration: this increases the signal-to-noise ratio appreciably and gives a direct estimate for the dwell time of sodium in the channel. However, this approach first requires a model for the transport of protons through the channel. It is known that protons pass through the gramicidin A channel by fast exchange reactions with water molecules that fill the pore (the Grotthus mechanism [16]). One therefore expects, for example, that binding sites for hydrogen ions inside the channel may be less well defined than for alkali ions. Keeping such limitations in mind, we attempt to theoretically describe the flux of protons by a 2S3B permeation model for sake of simplicity.

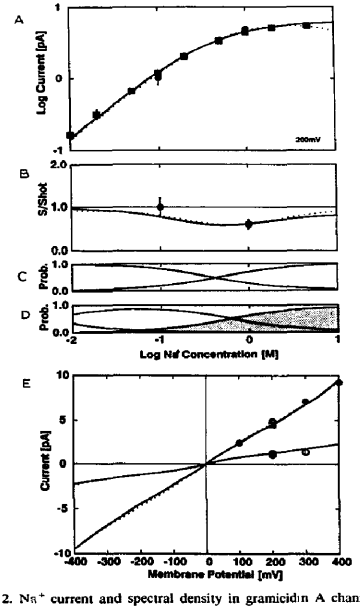

Fig. 2. Na^+ current and spectral density in gramicidin A channels, with theoretical curves from fitted parameter sets corresponding to 'weak binding' of Na^+ (solid curves; from Table II, column 4) and 'tight binding' (dotted curves; from Table II, column 2). (A) Logarithm of current at 200 mV as a function of Na^+ concentration. The circles are our data; the squares are data from Neher et al. [15] extrapolated to 200 mV assuming a linear current-voltage relationship. The solid and dotted curves are nearly superimposed. (B) The relative spectral density, normalized to the classical shot noise ($S_{shot} = 2\ i\ q$) shown with the theoretical curves for the two parameter sets. (C) Predicted probabilities of channel occupancy by zero or one ion for the 'weak binding' parameters. (D) Corresponding occupancy plot for the 'tight binding' parameters, with occupancy by two ions shown as the shaded region. (E) Current-voltage relationships in 0.1 M (open symbols) and 1.0 M NaCl (filled symbols). For all of the experimental data the two parameter sets give equally good fits.

TABLE II

Different sets of rate constants for Na^+ permeation through gramicidin A in s^{-1}

Rate	'Tight binding'		'Weak binding'	
	Ref. 3 [a]	fit [b]	Ref. 1 [c]	fit [d]
f_N/c	$3.0 \cdot 10^7$	$6.0 \cdot 10^7$	$1.9 \cdot 10^7$	$5.8 \cdot 10^7$
r_N	$3.0 \cdot 10^5$	$4.1 \cdot 10^5$	$1.2 \cdot 10^7$	$3.5 \cdot 10^7$
f_{NN}/c	$1.2 \cdot 10^8$	$6.8 \cdot 10^7$	$1.0 \cdot 10^4$	$9.6 \cdot 10^3$
r_{NN}	$4.0 \cdot 10^7$	$3.0 \cdot 10^7$	$1.0 \cdot 10^9$	$1.7 \cdot 10^9$
t_N	$> 3.0 \cdot 10^5$	$3.7 \cdot 10^7$	$2.0 \cdot 10^7$	$2.5 \cdot 10^7$

[a] After Urry et al. [3] derived from ^{23}Na-NMR experiments. For the translocation rate, r_N, only a lower limit could be given.

[b] Rate constants after Urry et al. [3] (column 1) adjusted to data as shown in Fig. 2. For the relative electrical position of the binding site in the electric field we assumed 0.13.

[c] After Finkelstein and Andersen [1].

[d] Rate constants after Finkelstein and Andersen [1] (column 3) adjusted to data as shown in Fig. 2.

Figs. 3A,B show the amplitude of single-channel currents and their normalized spectral densities of current noise as a function of proton concentration. These currents were measured in GMO/squalene membranes at 200 mV. The single-channel current saturates slightly at the highest attained concentration (320 mM); although the values of i are well fitted by this model, the spectral density shows an increase at high concentrations which cannot be accounted for by the model's prediction (thin curve in Fig. 3B).

One explanation for the increased noise with H^+ concentration would be a proton-dependent blockage of the channel, either directly via binding to the outside of the channel, or indirectly due to pH-dependent changes in the membrane. For example, GMO is unstable at low pH and its fission products, such as olic acid and glycerol, could give rise to a solvent effect on noise like that observed in GMO/decane membranes [8]. We attempted to explain the noise by mechanisms such as these by incorporating a concentration-dependent

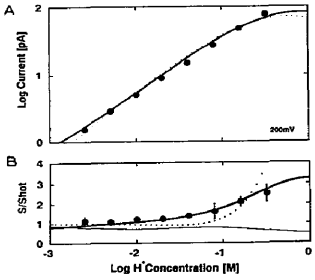

Fig. 3. Currents and spectral density in HCl solutions. (A) Logarithm of H^+ current as a function of H^+ concentration at 200 mV membrane potential. (B) Spectral density, normalized to the shot noise formula. The thin curve is the prediction of the simple four-state transport model (shown as heavy lines in the state diagram in (C)). The dotted curve is the best fit of a simple proton-block mechanism; the solid curve was a fit by the scheme shown in C, in which blocked states can be entered only if one or more protons are inside the channel. The fitted rates are $\alpha = 1.6 \cdot 10^3\ s^{-1}$ and $\beta = 8.1 \cdot 10^5\ s^{-1}$; the predictions for the concentration dependence of channel current by all three models are indistinguishable. Most data points were derived from single experiments; error bars indicate standard deviations of two or three independent measurements.

blocking reaction that did not depend on the actual channel state. The corresponding fit is shown as dotted curves in Figs. 3A and B, based on a blocking rate of $2.4 \cdot 10^3\ s^{-1} \cdot M^{-1}$ and an unblocking rate of $4.4 \cdot 10^5\ s^{-1}$.

A better description of the data resulted from assuming that the channel can become blocked (for about 1 μs at a time) if a hydrogen ion is inside the channel. The state model in Fig. 3C accounts for such a mechanism, in which all states except that of the empty channel [00] can be transformed into a blocked state. The resulting fit is shown as the solid curve in Figs. 3A and B, with $\alpha = 1.6 \cdot 10^3\ s^{-1}$ and $\beta = 8.1 \cdot 10^5\ s^{-1}$. We were, unfortunately, not able to record channel currents at lower pH values to further test this mechanism.

For our further calculations we nevertheless used the simple four-state model (Fig. 1A), which gives a good description of the H^+ conductance but which underestimates the spectral density. This did not greatly affect the interpretation of our Na^+ block experiments since we used relatively low H^+ concentrations.

Na^+ block experimens

Fig. 4 shows the mean currents and the relative spectral densities measured in mixtures of H^+ and Na^+. The probe current carried by 20 mM (open) and 80 mM H^+ (filled symbols), at 100 mV (A) and 200 mV (B) are plotted as a function of the added Na^+ concentration. The mean current as well as the spectral density was not very strongly affected by the presence of Na^+; this already suggests that sodium ions do not bind very

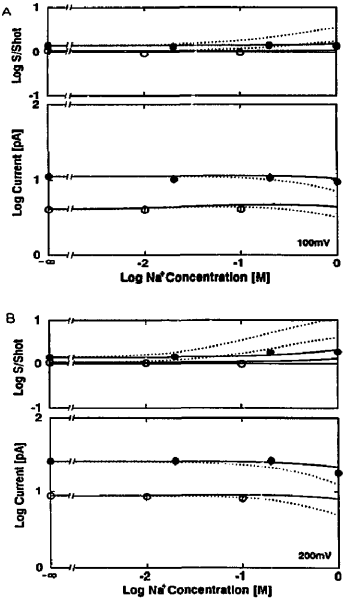

Fig. 4. Na^+ block experiments with first-order block theory. Changes in the current and noise in 20 mM HCl (open circles) and 80 mM HCl (filled circles) with added Na^+ at 100 mV (A) and 200 mV (B), respectively. The solid curves represent fits of the model-independent block reaction according to Eqns. 1–6. The association rate was taken to be diffusion-limited: $\lambda = 2.0 \cdot 10^7\ s^{-1}\ M^{-1}$. τ was determined by least-squares fit: $\tau = 8.4 \cdot 10^{-9}$ s (100 mV), $\tau = 12 \cdot 10^{-9}$ s (200 mV). The dotted curves show the clearly excessive noise increases and current decreases at high Na^+ concentrations that are predicted if the Na^+ dwell times τ are increased by a factor of 5.

tightly to a site inside the channel. The curves in the figure are least-squares fits to the data according to Eqns. 3 and 6, with the relative Na^+ current noise parameter $r_{Na} = 1$ and with the proton current noise parameter r_H set equal to r_H^0, the value determined in the absence of Na^+. The mobility ratio, ρ, was taken as a free parameter (initial value = 0.1). In a first simultaneous fit to all available data, ρ was estimated to be 0.138. Initially, the other free parameters λ and τ were then fitted to data grouped according to the membrane potential, with estimated values at 100 mV: $\tau = 2.6 \cdot 10^{-9}$ s, $\lambda = 1.2 \cdot 10^8\ s^{-1} \cdot M^{-1}$; at 200 mV: $\tau = 5.9 \cdot 10^{-9}$ s, $\lambda = 8.4 \cdot 10^7\ s^{-1} \cdot M^{-1}$. Since the curves are almost straight lines in the observed concentration range, it was necessary to constrain either λ or τ. Taking λ to be a typical diffusion-limited association rate, $2.0 \cdot 10^7\ s^{-1}$ we obtained $\tau = 8.4 \cdot 10^{-9}$ s (100 mV) and $\tau = 12 \cdot 10^{-9}$ s (200 mV). The affinities of 0.17 M^{-1} and 0.24 M^{-1}, respectively, are in close agreement with the results of Finkelstein and Andersen [1]. However, taking the 'weak binding' parameters of a four-state transport model (Table II, column 3), one obtains a dwell time that is approximately five times larger at 200 mV, yielding much higher noise spectral densities (see dotted curves in Fig. 4).

Predictions of the extended ion-transport model

The simple 'model-independent' theory is valid only when specific H^+–Na^+ interactions can be ignored, and when the probability of occupancy of the channel by Na^+ is low. The latter assumption almost certainly did not hold true for the data points obtained in 1 M NaCl. Further, the theory yields dwell times for ions in the channel, which are not the same as dwell times at the binding sites and therefore are not directly related to the dissociation rate. A more rigorous approach is to calculate the current and spectral density for the nine-state model (Fig. 1B) which accomodates directly the transport of both H^+ and Na^+ (see Ref. 8). This model explicitly contains the voltage dependence of ion transport and can therefore provide information about equilibrium rate constants.

Most of the rate constants in the nine-state model are the same as those in the four-state models for H^+ and Na^+ permeation alone. The constants for H^+ transport were taken from Table I and the adjusted rate constants for Na^+ transport in the cases of tight and weak binding were taken from Table II, columns 2 and 4, respectively. The other rates, mixed-occupancy configuration, were obtained by assuming that the association and dissociation of a second ion is independent of the species of the first bound ion, i.e., $f_{NH} = f_{NN}$, $r_{NH} = r_{NN}$ and $f_{HN} = f_{HH}$, $r_{HN} = r_{HH}$. The solid and dotted curves in Fig. 5 are predictions based on these sets of rate constants for 20 mM (Fig. 5A) and 80 mM H^+ (Fig. 5B). It is clearly seen that the model with tight sodium

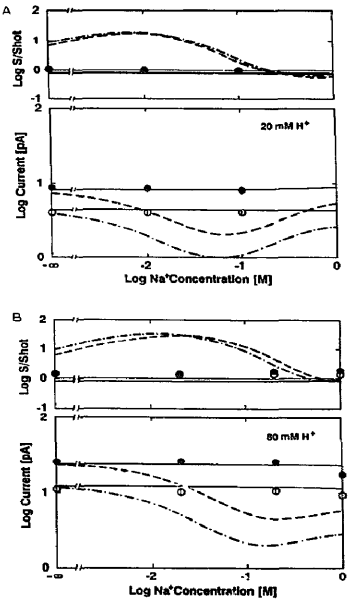

Fig. 5. Na^+ block experiments with predictions of a nine-state transport model. Normalized spectral density and logarithm of single-channel current as function of Na^+ concentration in 20 mM (A) and 80 mM HCl (B). Data obtained at 100 mV and 200 mV are shown as open circles and filled circles, respectively. The curves were calculated from the nine-state transport model (Fig. 1B) with independently-determined parameters. The H^+ transport parameters were from the fits in Fig. 3, and are given in Table I. Parameters for Na^+ transport were from column 4 of Table II ('weak binding' model; plotted as solid curves) or from column 2 of Table II ('tight binding' model; dashed and dashed-dotted curves).

binding predicts a reduction in mean current and a very large increase in noise spectral density that were not observed. The weak binding model predicts only small changes in current and noise, consistent with the observations. The deviations between the weak binding model and the data likely arise from the lack of a 'correct' transport model for proton permeation (see above). The rather strong discrepancy between data and model predictions at high Na^+ concentrations indicate the limitations of the model which does not account for specific H^+–Na^+ interactions either.

Discussion

Current and spectral density of sodium flux through the gramicidin A channel can be described by a two-site, three-barrier model. Such a description, however, is not unique; two very different sets of rate constants yield equally good characterizations of the conductance and noise data. To discriminate between these 'weak-binding' and 'tight-binding' models, we measured the mean value and spectral density of proton currents in the presence of various concentrations of Na^+, as well as in the absence of Na^+. These experiments are analogous to ones performed on Ca^{2+} channels [6], in which interruptions of a Na^+ or Li^+ current were used to measure the entry rate and dwell time of divalent cations in the channel. However as we expected, the Na^+ dwell times are far too short to produce resolvable interruptions in the single-channel current. The presence of Na^+ was seen to cause only a small decrease in the H^+ current, and a small open-channel noise. From the numerical fit of a simple first-order block mechanism to the data we obtained Na^+ dwell times of $8.4 \cdot 10^{-9}$ s and $12 \cdot 10^{-9}$ s and non-equilibrium Na^+ affinities of 0.17 M^{-1} and 0.24 M^{-1} at membrane potentials of 100 mV and 200 mV, respectively. These values agree well with the 'weak-binding' Na^+ transport rate constants of Finkelstein and Andersen [1].

A more general approach is to calculate the current and noise in a discrete transport system according to Frehland [11,12]. For this, a kinetic model of transport for H^+ as well as Na^+ was required. Assuming no species-specific interactions between ions in double occupancy of the channel, we combined our estimated H^+ transport rates with either the 'weak-binding' or the 'tight-binding' parameter sets and again found good agreement with the former set. The spectral density data discriminated very strongly against the tight-binding parameter set, which predicted spectral densities more than 20-fold larger than was observed.

Meanwhile, in the process of characterizing the H^+ permeation, we found a large excess noise at low pH that could not be described by the four-state ion-transport model alone. We obtained a good description of the concentration dependence of the noise by adding states to the model, allowing transitions into a blocked state (blocked time ≈ 1 μs) to occur, but only when the channel is occupied by H^+.

Our study of Na^+ permeation therefore confirms the view that Na^+ has a relatively low affinity for the gramicidin A channel, and that the apparent saturation of channel current at Na^+ concentrations above 1 M likely arises from the channel becoming occupied by one ion; double occupancy by Na^+ probably is a rare occurrence at accessible Na^+ concentrations. The relatively tight Na^+ binding constant of ≈ 30 M^{-1} determined by ^{23}Na-NMR [4] and by a combination of ^{205}Tl-NMR and cation competition [17] therefore appear not to reflect the binding of Na^+ in the permeation pathway of the functioning gramicidin A channel. We wonder if they might represent binding to another, nonconducting conformation of the gramicidin A protein.

Acknowledgements

The authors wish to thank Drs. G. Augustine and E. Neher for carefully reading the manuscript. This work was supported by grant NS21501 from the NIH. S.H.H. was partly supported by stipends of the German Academic Exchange Service (DAAD) and the Max-Planck-Gesellschaft.

References

1 Finkelstein, A. and Andersen, O.S. (1981) J. Membr. Biol. 59, 155–171.
2 Hladky, S.B. and Haydon, D.A. (1984) in Current Topics in Membranes and Transport (Stein, W.D., ed.), Vol. 21, pp. 327–372. Academic Press, Orlando.
3 Urry, D.W., Venkatachalam, C.M., Spisni, A., Läuger, P. and Khaled, M.A. (1980) Proc. Natl. Acad. Sci. USA 77, 2028–2032.
4 Urry, D.W., Trapane, T.L., Venkatachalam, C.M. and Prasad, K.U. (1986) Int. J. Quantum Chem., Quantum Biol. Symp. 12, 1–13.
5 Urry, D.W., Alonso-Romanowski, S., Venkatachalam, C.M., Trapane, T.L., Harris, R.D. and Prasad, K.U. (1984) Biochem. Biophys. Acta 775, 115–119.
6 Lansman, J.B., Hess, P. and Tsien, R.W. (1986) J. Gen. Physiol. 88, 321–347.
7 Decker, E.R. and Levitt, D.G. (1988) Biophys. J. 53, 25–32.
8 Heinemann, S.H. and Sigworth, F.J. (1988) Biophys. J. 54, 757–764.
9 Sigworth, F.J., Urry, D.W. and Prasad, K. (1987) Biophys. J. 52, 1055–1064.
10 Sigworth, F.J. (1985) Biophys. J. 47, 709–720.
11 Frehland, E. (1978) Biophys. Chem. 8, 255–265.
12 Frehland, E. (1980) Biophys. Chem. 12, 63–71.
13 Schottky, W. (1918) Ann. Phys. (Leipzig) 57, 541–567.
14 Heinemann, S.H. and Sigworth, F.J. (1988) Biophys. J. 53, 300a.
15 Neher, E., Sandblom, J. and Eisenman, G. (1978) J. Membr. Biol. 40, 97–116.
16 Levitt, D.G. (1978) Biophys. J. 22, 209–248.
17 Hinton, J.F., Fernandez, J.Q., Shungu, D.C., Whaley, W.L., Koeppe II, R.E. and Millett, F.S. (1988) Biophys. J. 54, 527–533.